Evaluation of drilling performance of waterjets for methane hydrate formation

Takayuki FUKUZAWA

1. INTRODUCTION

Methane hydrate (MH) is considered as one of a clean energy for preserving global environment. To develop MH economically, it is required that drilling equipment for MH formation is simple and less costly. To answer this requirement, a drilling method with waterjets has been proposed; Niino[1)] has developed a drilling equipment with waterjets and performed drilling experiments for the simulated MH formation using self spin nozzle in the laboratory. However, the nozzle used in the experiments was not suitable for drilling and the results were not enough to evaluate the drilling performance. Moreover, to reduce fluctuation of ambient pressure during the experiments, improvement was required in the method for supplying high pressure water.

In this study, to evaluate the drilling performance of waterjets for a simulated MH formation under high ambient pressure, I improved a method for supplying high pressure water to reduce the fluctuation of ambient pressure during experiments, developed a self spin nozzle suitable for drilling, measured rotational speed of the nozzle head and conducted drilling experiments with waterjets for the simulated MH formation using the improved system and the developed nozzle.

2. EXPERIMENTAL SYSTEM

2.1 Whole system

Fig. 1 shows a schematic diagram of the experimental system. The experimental system consists of a water tank 1, high pressure water pumps 2, 3, driving pressure control valves 4, 5, a switching valve unit 6, high pressure hoses 7, a dummy nozzle 8, small and large pressure vessels 9, 10, a pressure vessel for cyclone separator 11, an ambient pressure control valve 12, a nozzle feeding system 13, 14 and a measurement system 15 ~ 22. A specimen is placed in the large pressure vessel 9 and the nozzle system is attached in the small pressure vessel 10.

Tap water is supplied from the water tank 1 to the high pressure water pumps 2, 3. Driving pressure is adjusted to a designated value by the driving pressure control valves 4, 5. High pressure water is supplied to pressure vessels 9, 10 through both the switching valve unit 6 and the dummy nozzle 8. Ambient pressure is adjusted by the ambient

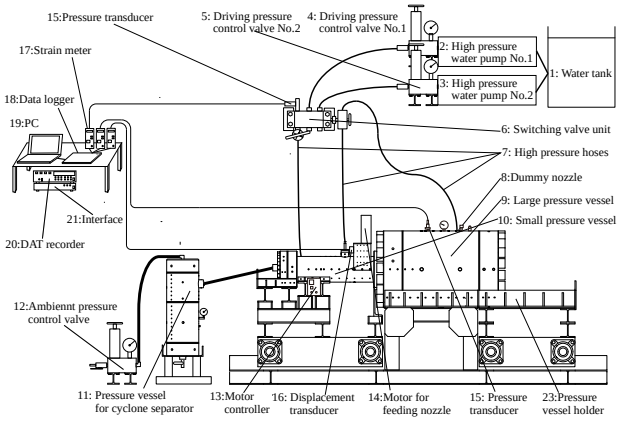

Fig. 1 Schematic diagram of experimental system.

pressure control valve 12, and nozzle feed is controlled by the nozzle feeding system 13, 14.

Fig. 2 shows the schematic diagram of the nozzle system in the measurement experiment of rotational speed. A cantilever (300 mm long × 12 mm wide × 8 mm thick) is fixed to the nozzle system by hose bands. A strain gauge is glued on the surface of the cantilever at 20 mm from the front edge of the cantilever. The cantilever is extended on the position of 170 mm from the front edge of the cantilever so that the waterjets jetted from a nozzle with an angle of 45° can only impinge the cantilever. The strains of the cantilever during the experiments were recorded by a DAT recorder. The data were divided into 12 parts, and the data of each part were analyzed by FFT to obtain the power spectrum.

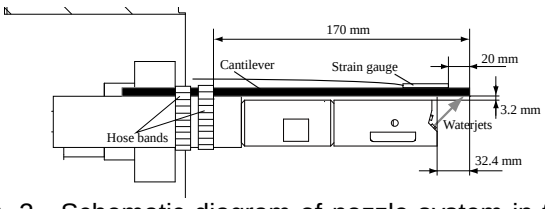

Fig. 2 Schematic diagram of nozzle system in the measurement experiment of rotational speed.

2.2 Dummy nozzle

The dummy nozzle with an equivalent diameter of the waterjets nozzle was used for reducing the fluctuation of ambient pressure during the experiments. Fig. 3 shows a schematic diagram of the dummy nozzle, and Fig. 4 shows the result of the fluctuation in ambient pressure during water jetting with the dummy nozzle. The driving

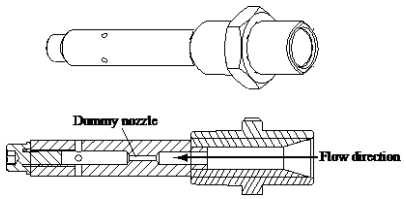

Fig. 3 Schematic diagram of dummy nozzle.

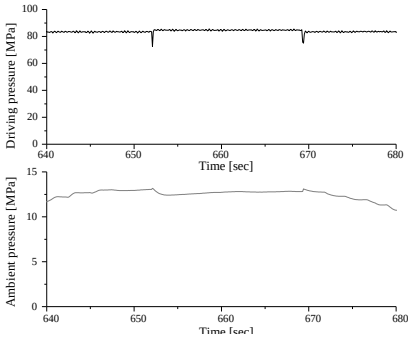

Fig. 4 Result of fluctuation in ambient pressure during water jetting with dummy nozzle (d_{45} / d_{15} = 1.4 / 1.4 mm, d_{dum} = 2.2 mm).

pressure is almost constant by supplying the high pressure water from the dummy nozzle before and after water jetting. As a result, the ambient pressure is almost constant during the experiments.

2.3 Self spin nozzle

Fig. 5 shows a schematic diagram of the self spin nozzle developed in this study. The self spin nozzle consists of two waterjets nozzles, a nozzle head, a body and a setscrew. The waterjets nozzles are attached to the front of the nozzle head eccentrically. Impinging angles of the waterjets nozzles are 45° and 15°, respectively. Accordingly, the nozzle head is rotated by the reaction forces induced by the water jetting. The size of the clearance between the walls of the cylinder and the body shaft is 55 ~ 74 μm. These hole and shaft are well polished to reduce the friction between the surfaces. Moreover, high pressure water leaking through the clearance can reduce the friction and cool off the temperature.

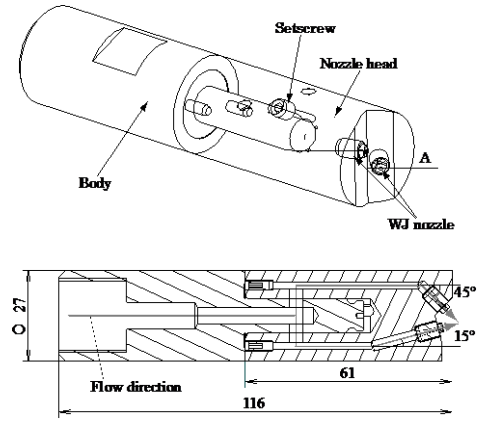

Fig. 5 Schematic diagram of self spin nozzle.

2.4 Specimen

Specimen used in this study is almost the same as that used by Niino[1]. This specimen closely simulates the physical and mechanical properties of in-situ MH formation by using CB (cement and bentonite). However, uniaxial strength of the specimen used in this study is about 50 % greater than that of the specimen used by Niino[1] due to longer curing time. Therefore, the borehole diameter obtained by the drilling experiment with waterjets for the specimens used in this study will be smaller than those obtained for the specimens used by Niino[1].

3. EXPERIMENTAL CONDITIONS

Table 1 shows experimental conditions for measuring rotational speed of the nozzle head (N). The purpose of this experiment is to investigate the effect of driving (p) and ambient (p_a) pressures on the rotational speed of the nozzle head (N).

Table 2 shows experimental conditions for drilling test. The purpose of this experiment is to investigate the effect of driving pressure (p), ambient pressure (p_a), nozzle diameter (d_{45} / d_{15}), nozzle feed rate (v), impinging angle and jetting time (t) on the drilling performance for the simulated MH formation under high ambient pressure (p_a). The diameters of waterjets nozzles are 1.0 mm, 1.2 mm and 1.4 mm. To evaluate the drilling performance with waterjets, a mold of the borehole was made of silicon rubber, and the length and the diameter of the mold of the borehole were measured.

4. RESULT AND DISCUSSION

4.1 Rotational speed of the nozzle head

Fig. 6 shows the power spectral density of the strain in the cantilever for different driving pressures (p) under ambient pressure (p_a) of 13 MPa. The peaks of the power spectral density at higher frequency indicate the inherent frequency of the cantilever, and the peaks at lower frequency indicate the rotational speed of the nozzle head (N). As the driving pressure (p) increases, the rotational speed of the nozzle head (N) increases. This is because the torque for the rotating nozzle head increases with the driving pressure (p). The relation between the rotational speed of the nozzle head (N) and the driving pressure (p) is almost linear. The rotational speed of the nozzle head (N) would be 0 for the driving pressure (p) of less than about 60 MPa, which may be minimum driving pressure (p) required to rotate the nozzle head under the ambient pressure (p_a) of 13 MPa.

Table 1 Experimental conditions for measuring rotational speed of the nozzle head (N).

Nozzle diameter, d_{45} / d_{15} (mm)	1.4 / 1.4	
Driving pressure, p (MPa)	65, 75, 80, 90, 95	85
Ambient pressure, p_a (MPa)	13	5, 7, 9,11, 13, 15
Impinging time, t (s)	130	

Table 2 Experimental conditions for drilling test.

Nozzle diameter, d_{45} / d_{15} (mm)	1.2 / 1.4			1.4 / 1.4				
Driving pressure, p (MPa)	70	85	95	65	75	85	90	95
Ambient pressure, p_a (MPa)	13			13	9, 13	6,13	13	
Nozzle feed length, l (mm)	260							
Nozzle feed rate, v (mm/s)	2, 3, and 5	5 and 10		5	5 and 10			

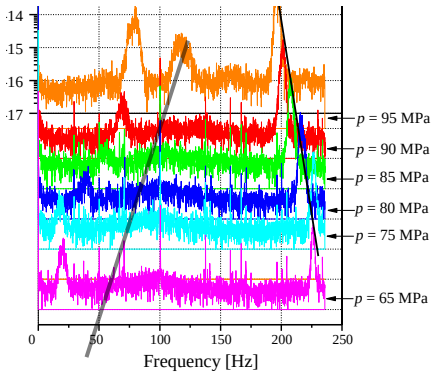

Fig. 6 Power spectral density of strain in cantilever for different driving pressures (p).

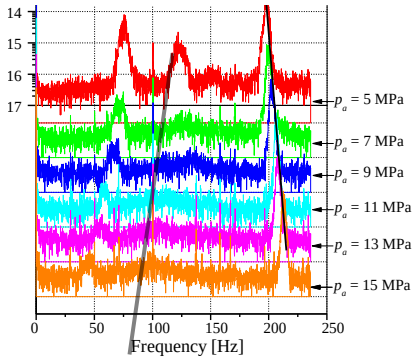

Fig. 7 Power spectral density of strain in cantilever for different ambient pressures (p_a).

Fig. 7 shows the power spectral density of the strain in the cantilever for the different ambient pressures (p_a). The peaks of the power spectral density at lower frequency indicate the rotational speed of the nozzle head (N) as those in Fig. 6. As the ambient pressure (p_a) increases, the rotational speed of the nozzle head (N) decreases. As the ambient pressure (p_a) increases, the clearance between the hole of the nozzle head and the body shaft decreases due to the contraction of the nozzle head. Accordingly, the friction of the sliding surfaces increases with the ambient pressure (p_a), which results in a decrease in the rotational speed.

4.2 Evaluation of waterjets drilling performance

Fig. 8 shows the photographs of the front edge of the silicon mold of the borehole when the nozzle head did not spin. Although the nozzle head did not spin, it was possible to feed the nozzle head toward the specimen by back and forth action. The diameters of both waterjets nozzles are 1.4 mm. As shown in Fig. 8, similar shapes are observed for two driving pressures (p). From these photographs, each depths of cut obtained by waterjets with impinging angles of 15° and 45° were measured. The depth of cut obtained by the waterjets nozzle with impinging angle of 45° (l_{45}) is much smaller than that obtained by the waterjets nozzle with impinging angle of 15° (l_{15}). This is because the length of entrance region in the upstream of the waterjets with impinging angle of 45° is only 1.6 mm, and is too small to rectify high pressure water flow.

Fig. 9 shows the photographs of the borehole walls obtained both by Niino[1)] (Fig. 9(a)) and in this study (Fig. 9(b)). Both impinging angles used by Niino[1)] are 45°. Spiral grooves are observed on the borehole wall obtained by Niino[1)] (Fig. 9(a)). Accordingly, strong spiral flow was induced in the annulus. As a result, the spiral grooves are formed by the erosion due to the impingement of cuttings on the borehole wall. On the contrary, here grooves are not observed in the wall obtained in this study (Fig. 9(b)). This is because the strong spiral flow was not induced by the nozzle of impinging angles of 45° and 15°.

Fig. 10 shows the relation between the driving pressure (p) and the mean diameter of the borehole (d). The mean diameter of the borehole (d) obtained by the nozzle feed rate (v) of 5 mm/s is greater than

that obtained by the nozzle feed rate (v) of 10 mm/s. This is because the impinging time of waterjets per unit length in nozzle feed rate (v) of 5 mm/s is greater than that in nozzle feed rate (v) of 10 mm/s.

The mean diameter of the borehole (d) obtained by nozzle diameters (d_{45} / d_{15}) of 1.4 / 1.4 mm is much smaller at driving pressure (p) of 95 MPa than those obtained at other driving pressures (p). This is because the rotational speed of the nozzle head (N) is about 4,800 rpm at driving pressure (p) of 95 MPa and accordingly, the traverse velocity of the waterjets impinging on the borehole wall seems to be too large.

The mean diameter of the borehole (d) obtained by nozzle diameters (d_{45} / d_{15}) of 1.4 / 1.4 mm is smaller than that obtained by nozzle diameters (d_{45} / d_{15}) of 1.2 / 1.4 mm under high driving pressures (p) while the flow rate of waterjets increases with nozzle diameter. This is because the rotational speed of the nozzle head (N) is too large in nozzle diameters (d_{45} / d_{15}) of 1.4 / 1.4 mm under these high driving pressures (p). Thus, the drilling performance with waterjets strongly depends on the rotational speed of the nozzle head (N).

The mean diameter of the borehole (d) obtained by nozzle diameters (d_{45} / d_{45}) of 1.0 / 1.0 mm is the greatest in this study. The difference of the mean diameter of the borehole (d) between that obtained by nozzle diameters (d_{45} / d_{45}) of 1.0 / 1.0 mm and that obtained by nozzle diameters (d_{45} / d_{15}) of 1.4 / 1.4 mm increases with the nozzle feed rate (v). This is because the depth of cut obtained by nozzle diameters (d_{45} / d_{45}) of 1.0 / 1.0 mm with the impinging angle of 45°is greater than that obtained by nozzle diameters (d_{45} / d_{15}) of 1.4 / 1.4 mm for high nozzle feed rate (v).

Fig. 11 shows the relation between the ambient pressure (p_a) and the mean diameter of borehole (d). Since the impinging force of waterjets decreases with the ambient pressure (p_a), it was expected that the mean diameter of borehole (d) decreases with the ambient pressure (p_a). However, the mean diameter of the borehole (d) increases with the ambient pressure (p_a). This is because the rotational speed of the nozzle head (N) decreases with the ambient pressure (p_a), and the driving performance increases with the ambient pressure (p_a).

5. CONCLUSION

Main results obtained in this study can be summarized as follows:

1) The fluctuation of the ambient pressure (p_a) during the experiments was reduced by supplying high pressure water from the dummy nozzle.

2) The self spin nozzle suitable for drilling was developed.

3) The rotational speed of the nozzle head (N) increases with driving pressure (p), and decreases with ambient pressure (p_a).

4) The mean diameter of borehole (d) mainly depend on the rotational speed of the nozzle head (N), which decreases the performance of the nozzle system.

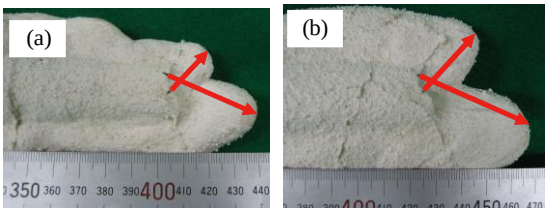

Fig. 8 Photographs of front edge of silicon mold of the borehole ((a) p = 85 MPa and (b) p = 93 MPa).

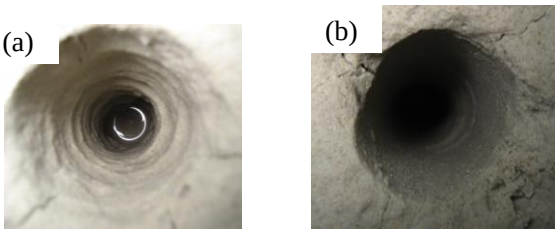

Fig. 9 Photographs of borehole wall ((a) p = 85 MPa, d_{45} / d_{45} = 1.0/1.0 mm and (b) p = 85 MPa, d_{45} / d_{15} = 1.4/1.4 mm).

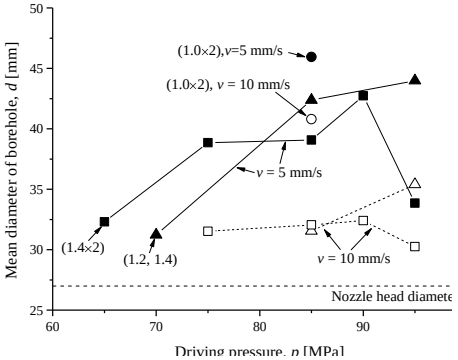

Fig. 10 Relation between driving pressure (p) and mean diameter of borehole (d).

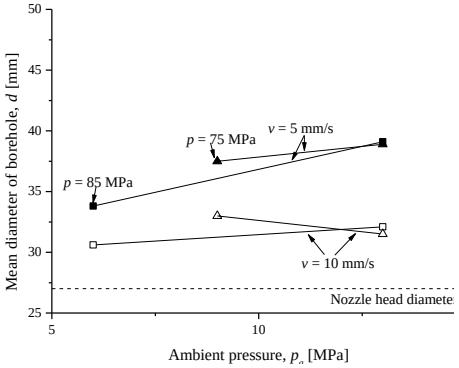

Fig. 11 Relation between ambient pressure (p_a) and mean diameter of borehole (d).

REFERANCE

[1] Niino, 2006, An experimental study on drilling of methane hydrate formation by high pressure water jet, Tohoku Univ. Master thesis.